AGU PUBLICATIONS

JGR

Journal of Geophysical Research: Oceans

RESEARCH ARTICLE

10.1002/2014JC010246

Key Points:

- Quantification of the thermocline water mass distribution in the Coral Sea
- Determination of the pathways of the thermocline water masses in the Coral Sea
- Relationships with the dynamics of the main currents

Supporting Information:

- Description of supporting figure files
- Figure S1
- Figure S2
- Figure S3
- Figure S4
- Figure S5
- Figure S6
- Figure S7
- Figure S8
- Figure S9
- Figure S10
- Figure S11
- Figure S12
- Figure S13
- Figure S14

Correspondence to:

F. Gasparin,
fgasparin@ucsd.edu

Citation:

Gasparin, F., C. Maes, J. Sudre, V. Garcon, and A. Ganachaud (2014), Water mass analysis of the Coral Sea through an Optimum Multiparameter method, *J. Geophys. Res. Oceans*, *119*, 7229–7244, doi:10.1002/2014JC010246.

Received 16 JUN 2014
Accepted 12 AUG 2014
Accepted article online 19 AUG 2014
Published online 29 OCT 2014

Water mass analysis of the Coral Sea through an Optimum Multiparameter method

Florent Gasparin[1], Christophe Maes[2], Joel Sudre[3], Veronique Garcon[3], and Alexandre Ganachaud[2]

[1]Scripps Institution of Oceanography, University of California, San Diego, La Jolla, California, USA, [2]Institut de Recherche pour le Développement, UMR5566-LEGOS, UPS (OMP-PCA), Toulouse, France, [3]CNRS, UMR5566-LEGOS, UPS (OMP-PCA), Toulouse, France

Abstract A water mass analysis of the Coral Sea thermocline waters provides a description of their distribution, pathways and mixture based on recent oceanographic cruises in this region of strong western boundary currents. The Optimum Multiparameter method is used to determine the relative contribution of core water masses based on their measured temperature, salinity and dissolved oxygen. The thermocline waters, carried by the broad South Equatorial Current (SEC), are essentially composed of four core water masses of different origins. Coming from the south, the *South Pacific Tropical Water South* (SPTWS, $\sigma = 25.3$ kg m^{-3}) and the *Western South Pacific Central Water* (WSPCW, $\sigma = 26.3$ kg m^{-3}) enter the Coral Sea by the channel between the island of New Caledonia and the Vanuatu archipelago. Coming from the north, the *South Pacific Tropical Water North* (SPTWN, $\sigma = 24.5$ kg m^{-3}) and the *Pacific Equatorial Water* (PEW, $\sigma = 26.3$ kg m^{-3}) flow north of Vanuatu. The upper thermocline water that exits the Coral Sea equatorward, is mainly composed of SPTWN carried by the New Guinea Coastal Undercurrent. In contrast, upper thermocline waters exiting the Coral Sea poleward, in the East Australian Current, is dominated by SPTWS. The relative contributions are different in the lower thermocline where WSPCW dominates both western boundary currents. This refined description is consistent with the dynamics of the main currents, with a very strong depth dependence in the partitioning of incoming SEC waters.

1. Introduction

In the tropical southwest Pacific, thermocline waters, referring to the depth range of 100–400 m, can be traced back to the center of the South Pacific subtropical gyre. These follow a peculiar pathway, first carried westward by the South Equatorial Current (SEC) into the Coral Sea; then arriving at the Australian coast, splitting, with the southern branch running poleward along the Australian coast creating the East Australian Current (EAC) and the north branch forming a boundary current that flows equatorward into the Solomon Sea, and ultimately feeding into the equatorial current system [*Tsuchiya et al.*, 1989]. Because of its potential influence on equatorial surface waters and on the characteristics of the El Niño Southern Oscillation (ENSO) on decadal timescales [*Gu and Philander*, 1997], this circulation pathway has led to a major research effort, the Southwest Pacific Ocean Circulation and Climate Experiment (SPICE) (A. Ganachaud et al., Ocean circulation of the southwest pacific: New insights from the southwest Pacific Ocean and climate experiment (SPICE), submitted to *Journal of Geophysical Research*: *Oceans*, 2014).

The ocean dynamics in the southwest Pacific are controlled by a branching of the SEC, the westward limb of the south Pacific subtropical gyre that extends from the equator to 30°S (Figure 1). Upon its arrival near the dateline, the SEC divides around the major islands and reefs of Fiji (18°S, 178°E), the Vanuatu archipelago (16°S, 168°E), and New Caledonia (22°S, 165°E). It creates a complex system of western boundary currents (WBCs) and zonal jets. The main two jets entering the Coral Sea are the *North Vanuatu Jet* (NVJ), which is broad and shallow (0–500 m depth), and the narrow and deep (0–1500 m depth) *North Caledonian Jet* (NCJ) [*Webb*, 2000; *Gourdeau et al.*, 2008] which originates from the *East Caledonian Current* (ECC) along the east coast of New Caledonia [*Gasparin et al.*, 2011]. Observations [*Andrews and Clegg*, 1989; *Sokolov and Rintoul*, 2000; *Gasparin et al.*, 2012; *Davis et al.*, 2012; *Kessler and Cravatte*, 2013a] and numerical models [*Melet et al.*, 2010] suggest two thermocline water pathways between the Coral Sea and the equator: one is via the WBC that flows northward along the northeast coasts of Australia, around the Gulf of Papua and into the

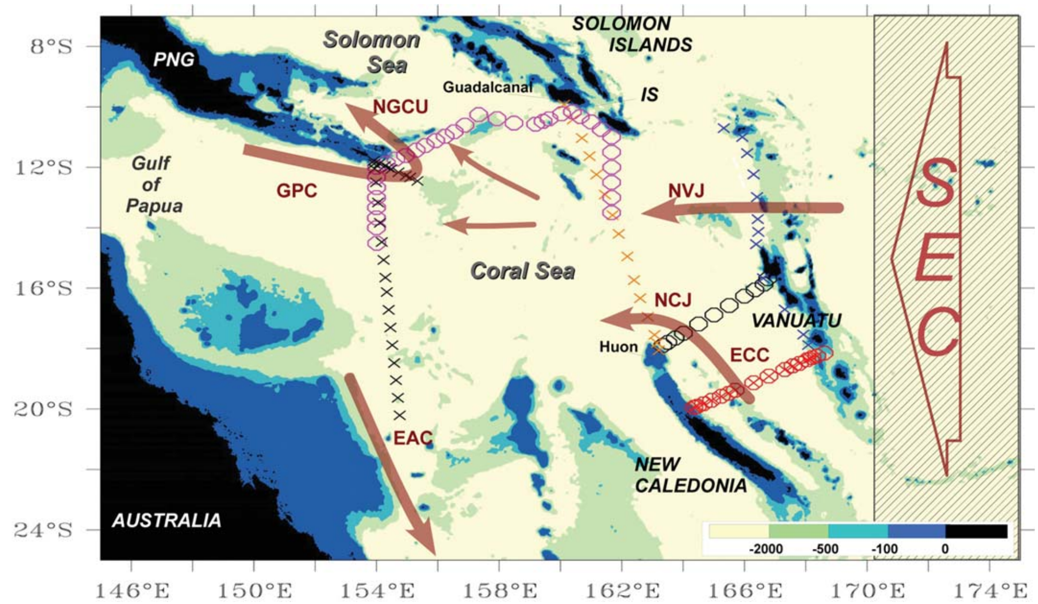

Figure 1. Location of hydrographic stations from seven oceanographic cruises used in the analysis (black-× = WOCE-P11 (Jun 1993), red-○ = WOCE-P21 (Jun 1994), black-○ = SECALIS-1 (Jul 2004), orange-× = SECALIS-3 (Jul 2005), blue-× = SECALIS-4 (Dec 2006), purple-○ = FLUSEC-1 (Aug 2007), red-× = P21-REVISIT (Jun 2009)). The currents are indicated by the arrows. Water mass cores are defined from within the hatched area. The 100 m, 500 m and 2000 m levels are indicated by blue/green colors. Country/Current/Strait names are indicated as follows: Indispensable Strait (IS); Papua New Guinea (PNG); South Equatorial Current (SEC); East Caledonian Current (ECC); North Caledonian Jet (NCJ); North Vanuatu Jet (NVJ); Gulf of Papua Current (GPC); New Guinea Coastal Undercurrent (NGCU); East Australian Current (EAC).

Solomon Sea; the second is a direct inflow from the northern Coral Sea to the southern Solomon Sea (two bifurcating arrows in the middle of the Coral Sea, Figure 1).

In the southwest Pacific, thermocline water masses are mainly composed of *Central Waters* found throughout the tropics and subtropics and of *Equatorial Waters* mainly located in the equatorial band between 10°S and 10°N [*Sverdrup et al.*, 1942; *Tomczak and Hao*, 1989]. *Tomczak and Godfrey* [2003] distinguish two density layers within the thermocline. At around 200 m ($\sigma \sim 25$, here and in the following, σ is the relative density defined as the absolute density minus 1000 and is expressed in kg m^{-3}), *Tropical Waters* identify the subsurface salinity maximum waters originating from two different surface salinity maxima [*Donguy and Henin*, 1977; *Donguy*, 1994]. A first salinity maximum originates from the Central Pacific near French Polynesia (18°S, 150°E), and is carried by the SEC to the Coral Sea at density $\sigma = 24.5$; this warm (20°C < T < 25°C), salty (S > 35.7) and oxygenated ($O_2 \sim 140$ μmol l^{-1}) water mass is known as the *South Pacific Tropical Water North (SPTWN)* [*Wyrtki*, 1962; *Sokolov and Rintoul*, 2000; *Qu and Lindstrom*, 2002]. Further south, a second subsurface salinity maximum is observed and arising from the Subtropical Convergence zone around New Zealand between 30°S and 40°S [*Sokolov and Rintoul*, 2000]. With a slightly larger density ($\sigma = 25.2$), this water mass, called *South Pacific Tropical Water South (SPTWS)*, is slightly colder (16°C < T < 22°C), slightly fresher (S$\sim$35.6) and more oxygenated ($O_2 \sim 180$ μmol l^{-1}) than the SPTWN [*Wyrtki*, 1962; *Sokolov and Rintoul*, 2000; *Qu and Lindstrom*, 2002]. Arriving in the Coral Sea with similar Temperature-Salinity characteristics, these two water masses can be distinguished using their oxygen concentration characteristics [*Tomczak and Hao*, 1989].

At deeper levels (around 300–400 m, $\sigma = 25.5$–27), the "lower thermocline" is mainly composed of *Western South Pacific Central Water (WSPCW)* coming from the south and the *Pacific Equatorial Water (PEW)* originating from the East. The WSPCW is formed in the Subtropical Convergence around New Zealand, and subducted through Ekman pumping and then transported toward the tropics along its isopycnal [*Roemmich and Cornuelle*, 1992; *Sprintall and Tomczak*, 1993; *Tsubouchi et al.*, 2007; *Holbrook and Maharaj*, 2008]. This water is salty (S $\sim$35.3), and highly oxygenated ($\sim$180 μmol l^{-1}) [*Sokolov and Rintoul*, 2000; *Qu et al.*, 2009]. The less-documented PEW is formed in the tropics in the Central Pacific following the equatorial current system [*Tomczak and Hao*, 1989]. This water mass is fresher ($\sim$35.15) and less oxygenated ($\sim$110 μmol l^{-1}). WSPCW and PEW have a temperature range close to 13–14°C [*Tomczak and Hao*, 1989; *Sokolov and Rintoul*, 2000; *Qu et al.*, 2009].

Table 1. Oceanographic Cruises Considered in the Study[a]

Cruise	Date	Context	References
WOCE-P11	Jun 1993	WOCE	*Sokolov and Rintoul* [2000]
WOCE-P21	Jun 1994	WOCE	*Tsimplis et al.* [1998]
SECALIS-1	Jul 2004	SPICE	*Gasparin et al.* [2011]
SECALIS-3	Jul 2005	SPICE	*Gourdeau et al.* [2007a, 2008]
SECALIS-4	Nov 2006	SPICE	*Gourdeau et al.* [2007b]
FLUSEC-1	Aug 2007	SPICE	*Maes et al.* [2008]; *Gasparin et al.* [2012]
P21-REVISIT	Jun 2009	WOCE	*Uchida et al.* [2011]

[a]For each cruise, Conductivity-Temperature-Depth-Oxygen (CTD-O_2) profiles provide temperature, salinity and dissolved oxygen concentration from the surface to at least 2000 m depth with respective accuracy of 0.005°C, 0.001 and 1 μmol kg^{-1}, according to the WOCE standards (CTD sections are provided in the supporting information Figures S1–S7). Only selected hydrographic stations are used to obtain closed sections enabling an estimate of the exchange between the Coral Sea and the surrounding regions.

In this paper, we use an Optimum Multiparameter (OMP) analysis to analyze Coral Sea thermocline waters and describe their distribution, pathways and mixture following the main SEC pathways from the eastern Coral Sea and its bifurcation toward the equator and the pole (Figure 1). The main objective of this paper is to reassess the distribution of the different thermocline water masses using an OMP analysis with recent CTD-O_2 data, in combination with earlier hydrographic data, and to quantify the relative contributions, in comparison with the classical approach based on temperature/salinity/oxygen diagrams.

The paper is organized as follows: Hydrographic data and the OMP method are described in section 2. Water masses are defined in this section, and a range of experiments are described that allow for the determination of the relative contribution of each water mass. In section 3, the distribution of each water mass within the thermocline is determined along the SEC pathways. Finally, a summary and discussion are presented in section 4.

2. Optimum Multiparameter Method

The OMP analysis, introduced by *Tomczak and Large* [1989], allows the mixture ratios of water masses to be determined through the use of their hydrographic properties. Here we consider seven oceanographic cruises (Table 1) completed between 1993 and 2009 during the *WOCE* and *SPICE* programs. The eastern Coral Sea was sampled by cruises WOCE-P21, SECALIS-1 and P21-REVISIT in the New Caledonia-Vanuatu channel and by SECALIS-4 and FLUSEC-1 north of Vanuatu (Figure 1). The middle of the Coral Sea between New Caledonia and the Solomon islands (Guadalcanal) was sampled by SECALIS-3. Further west, the entrance of the Solomon Sea in the western Coral Sea was sampled by FLUSEC-1 and WOCE-P11. The OMP is an inverse method based on a system of linear equations in which contributions (%) of a given Source Water Type (SWT, specific properties characterizing a water mass) are fitted to the observed water properties which are, for our cruises, potential temperature (θ), salinity (S), and oxygen (O). Given the characteristics of each SWT$_i$ (θ_i, S_i, O_i), the OMP resolves the following system of property conservation equations:

$$\begin{cases} x_1.\theta_1+x_2.\theta_2+x_3.\theta_3+x_4.\theta_4=\theta obs+R_\theta \\ x_1.S_1+x_2.S_2+x_3.S_3+x_4.S_4=Sobs+R_S \\ x_1.O_1+x_2.O_2+x_3.O_3+x_4.O_4=Oobs+R_O \\ x_1+x_2+x_3+x_4=1+R_M \end{cases} \quad (1)$$

where $\boldsymbol{x_i}$ is the contribution (%) of each SWT$_i$ (here using four SWT), R are residuals, "obs" refers to observed properties from our data. The last equation is mass conservation.

The system of equations can be written in a matrix form

$$\mathbf{Gx}-\mathbf{d}=\mathbf{R} \quad (2)$$

where **G** is the SWT definition matrix, **d** is the observation vector, **x** is the solution vector (ratios of each SWT) and **R** is the residual vector.

Each equation is weighted by the standard deviation ω of each property, following *Maamaatuaiahutapu et al.* [1992]. The weights depend on two components that are the measurement errors and the arbitrariness in

Table 2. Source Water Type (SWT) of Each Water Mass Considered in the Experiments[a]

	G						
	Surface	Upper Thermocline		Lower Thermocline		Intermediate	$W = \omega^2 I$
	TSW	SPTWN	SPTWS	WSPCW	PEW	AAIW	ω
σ	>24	~24.5	~25.3	~26.3	~26.3	~27	
T (°C)	28	22	19.5	14.5	14.5	5.5	0.25
S	34.5	35.9	35.65	35.25	35.13	34.45	0.07
O_2 (μmol kg^{-1})	200	120	175	180	115	180	5
M ($\omega_i X_i = 1$)	1	1	1	1	1	1	0.01

[a]Water masses characteristics and ω is the standard deviation of each property. **G**, **W** and **I** are respectively the SWTs matrix, the weighting matrix and the identity matrix (see section 2). TSW = Tropical Surface Water. SPTWS = South Pacific Tropical Water South/ SPTWN = South Pacific Tropical Water North. WSPCW = Western South Pacific Central Water/PEW = Pacific Equatorial Water. AAIW = Antarctic Intermediate Water.

SWT parameter choices. Our weights are therefore similar to those of *Maamaatuaiahutapu et al.* [1992] used in the South Atlantic. In practice, our weights (Table 2) are expressed in the units of each parameter, so that the relative weights are not directly comparable with the *Tomczak and Large* [1989] weights. But the resulting T, S and mass conservation equations are given a much higher weight than oxygen. As an independent test, we did a sensitivity experiment based on subtropical thermocline weights as in *Tomczak and Large* [1989], and found no significant changes in the distribution of water masses.

The system is solved by a least square method to minimize the residuals:

$$\mathbf{R^T R} = (\mathbf{Gx} - \mathbf{d})^{\mathbf{T}}\ \mathbf{W^{-1}}\ (\mathbf{Gx} - \mathbf{d}) \tag{3}$$

where *T* is the transposed matrix operator and W^{-1} is the the diagonal weight matrix (covariance matrix) *W* (= $\omega^2 I$, where *I* is the identity matrix).

Residuals (3) provide an assessment of the quality of the solution [*Tomczak and Large*, 1989; *Poole and Tomczak*, 1999]. A mass conservation residual lower than 5–7% is a criterion used in common OMP practice for the reliability of the solution [*Poole and Tomczak*, 1999; *Budillon et al.*, 2003]. However, we will use a different criterion based on the 90% of confidence if the residuals follow the χ^2 distribution. In this case, the weighted residuals should be lower than 0.25 [*Maamaatuaiahutapu et al.*, 1992].

Following *Maamaatuaiahutapu et al.* [1992], 100 perturbation experiments were performed to assess the robustness of the solution by randomly varying each property of SWT (matrix **G**) within its standard deviation ω based on observed variability (Table 2). The standard deviation of the solutions was found to be very low (<10% of the mean), and so in the following we present only the average of these perturbation experiments. The typical error solution is considered as 10%.

2.1. Water Mass Properties and Experiments

SWT characteristics correspond to the aforementioned water masses at the entrance of the Coral Sea, near 170°E (Table 2, hatched area in Figure 1). At the surface (above $\sigma = 23.5$), tropical atmospheric conditions produce *Tropical Surface Water* (TSW) (indicated by the "◇" symbols in Figure 2) which are warm (>25°C), fresh (<35.00), and saturated in oxygen (~190–200 μmol kg^{-1}) and are located above 200 m depth.

The SPTWS and the SPTWN (~100–300 m depth) correspond to the aforementioned salinity maxima (squares in Figure 2). This North-South contrast is related to the regional oceanic circulation: around 163°E between New Caledonia and Solomon islands, a clear front between 15°S and 16°S is observed down to $\sigma = 27$ (Figure 3), separating the zonal NCJ (18°S–16°S) and NVJ (north of 15°S) (Figure 1). Such a front was also observed on glider transects [*Gourdeau et al.*, 2008]. North of 12°S, low oxygen anomalies in both thermocline and intermediate waters mark an inflow from the Indispensable Strait [*Gasparin et al.*, 2012].

Between $\sigma = 25.5$ and $\sigma = 26.5$ (~300–600 m depth), the salinity is higher between New Caledonia and Vanuatu than north of 16°S (Figure 2). There is also a front in oxygen at 16.5°S in that same density range (Figure 3) with high oxygen (160–185 μmol kg^{-1}) on the southern side and low oxygen (115–160 μmol kg^{-1}) on the northern side. The salty and oxygenated water of the south represents the WSPCW, while the fresher and less-oxygenated water of north represents the PEW ("•" in Figure 2) [*Tomczak and Hao*, 1989].

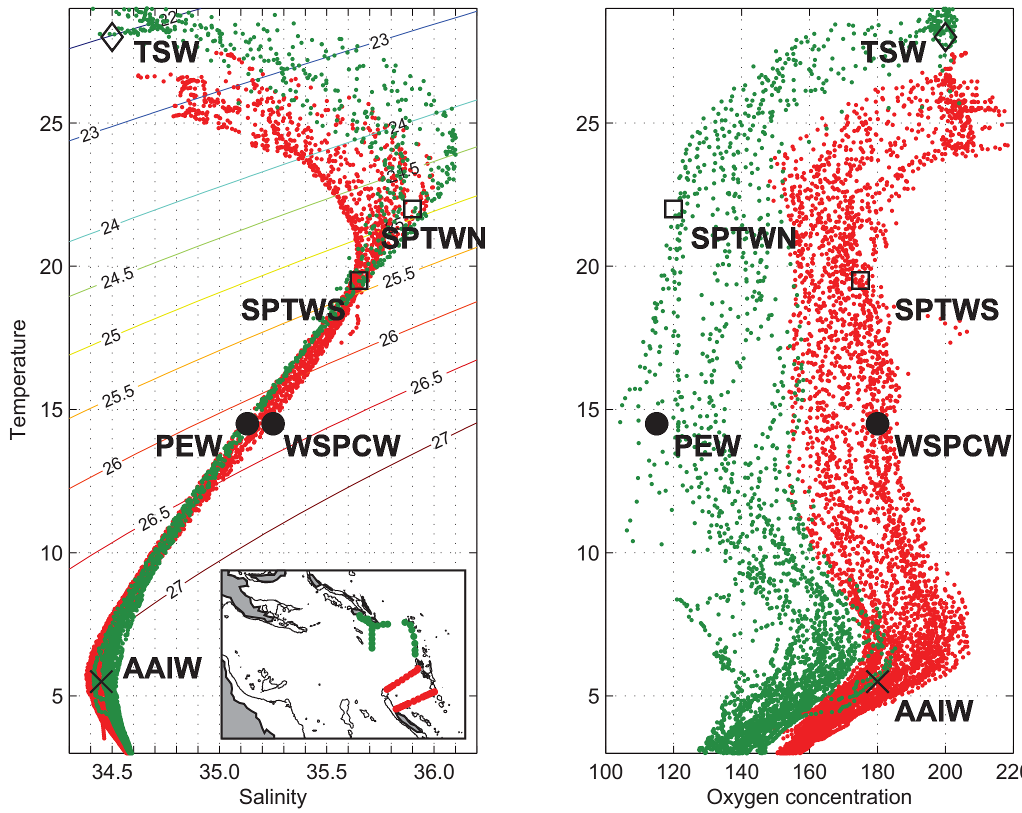

Figure 2. Temperature-Salinity (T-S) and Temperature-Oxygen Concentration (T-O_2) diagrams from hydrographic stations located in the northern part (in green, stations from the SECALIS-4/FLUSEC-1 cruises) and in the southern part of the Coral Sea (in red, stations from the WOCE-P21/SECALIS-1/P21-REVISIT cruises). Temperature is expressed in °C, and oxygen concentration in μmol kg^{-1}. The black signs indicate the properties of the water masses used in the OMP ("◇" = TSW, "□" = SPTWS and SPTWN, "•" = WSPCW and PEW, "×" = AAIW). Geographic station positions are indicated in the inset.

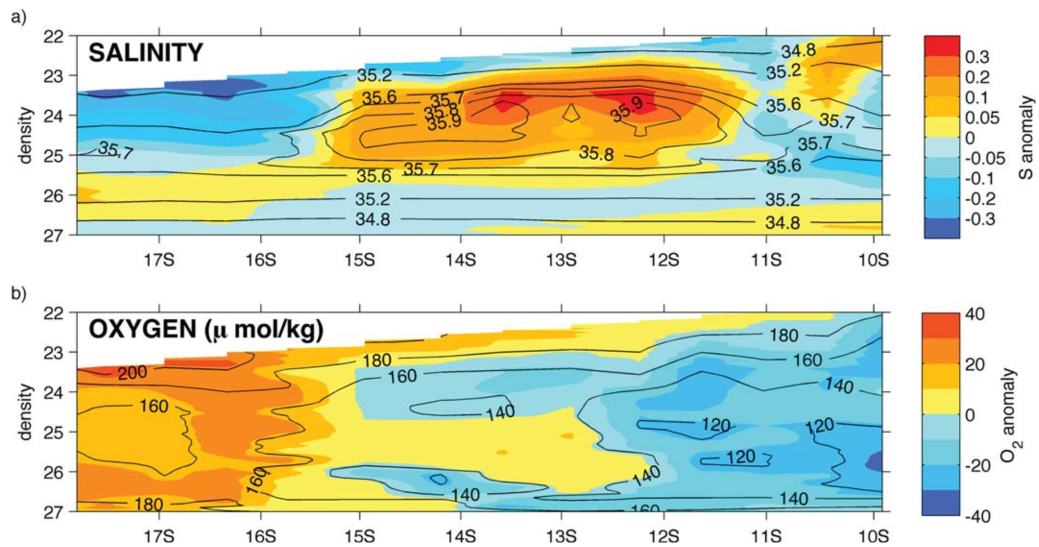

Figure 3. Water mass properties between Huon (North of New Caledonia) and Guadalcanal (East of the Solomon Islands); SECALIS-3 cruise; (a) salinity and (b) oxygen concentration (in μmol kg^{-1}) as a function of latitude and density (m^3 kg^{-1}). Contour lines show the full values while isopycnals anomalies from the mean of the section stations are indicated by color.

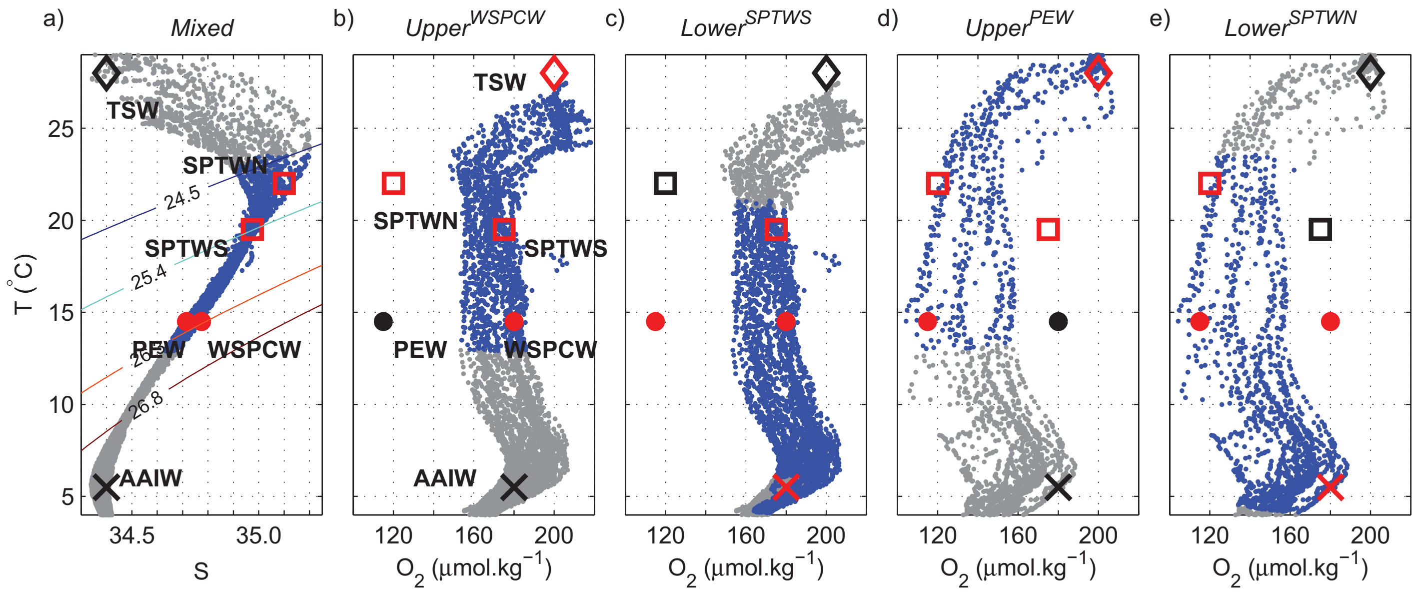

Figure 4. The five experiments used in the analysis illustrated by a TS diagram (a) *Mixed* experiment, and O_2T diagrams (b) *Upper*^{WSPCW}, (c) *Lower*^{SPTWS}, (d) *Upper*^{PEW}, (e) *Lower*^{SPTWN} for sections in the eastern Coral Sea (WOCE-P21/SECALIS-1/P21-REVISIT (Figures 4a–4c) and SECALIS-4/FLUSEC-1 (Figures 4a, 4d, and 4e)). SWTs are indicated by the large symbols, as indicated in Figures 4a and 4b (in red, the ones included in the inversion) and properties that were determined reliably through the inversion (mass residual lower than 1.4) are indicated in blue.

Below $\sigma = 26.5$ (below 500 m depth), the lower salinity and higher oxygen result from the influence of the fresh and oxygenated *Antarctic Intermediate Water* (AAIW) coming from the south ("×" in Figure 2) [*Sokolov and Rintoul*, 2000; *Qu and Lindstrom*, 2004; *Maes et al.*, 2007].

The system (2) is under-determined for six water masses as we have only limited to three parameters plus mass conservation (1). It requires the use of subsets of four SWTs. We first use a *Mixed* configuration which considers the four thermocline SWTs (Figure 4a and Table 3). This is used as a first guess of water mass contribution because (i) reliable solutions are only found in a thin layer ($\sigma = 24.5$–26.3, blue dots in Figure 4) due to the relatively close characteristics of the thermocline SWTs. (ii) The Mixed experiment can not resolve (with low residuals) the surface (0–200 m) and intermediate (400–600 m) levels because we miss the contribution of the TSW/AAIW to the mixture. We do not present these Mixed configurations as they are only used to guide our configuration choices, but they are found in the supporting information (Figures S8–S12).

To go beyond this limitation, we adopt the *vertical stacking* strategy which enables us to separate the equation system (2) into different subsystems [*Sudre et al.*, 2011]. We use a series of four configurations, as shown on Figure 4 and Table 3. Using TSW, we can focus on Tropical Waters contributions (SPTWS/SPWTN, upper part of the thermocline) with either the *Upper*^{WSPCW} (no PEW) or the *Upper*^{PEW} (no WSPCW) (Figures 4b and 4c). For these two experiments, we focus on areas where WSPCW or PEW contributions are expected to be low. For instance, the *Upper*^{WSPCW} experiment (where PEW is not considered) is applied in the New Caledonia-Vanuatu channel, suspected to have low PEW contribution. This hypothesis is then validated by looking at the PEW contribution with the *Lower*^{SPTWS} experiment (No SPTWN). We use the perturbation experiments to assess the robustness of this experimental setting.

Table 3. Experimental Settings[a]

Experiment	SWT	Hypothesis
Mixed	SPTWS-SPTWN-WSPCW-PEW	
Upper^{WSPCW}	TSW-**SPTWS-SPTWN**-WSPCW	No PEW contribution
Upper^{PEW}	TSW-**SPTWS-SPTWN**-PEW	No WSPCW contribution
Lower^{SPTWS}	SPTWS-WSPCW-PEW-AAIW	No SPTWN contribution
Lower^{SPTWN}	SPTWN-**WSPCW-PEW**-AAIW	No SPTWS contribution

[a]Column 1 refers to the experiment label; followed by the SWTs used and underlying hypotheses. The *Mixed* experiment considering the four thermocline SWTs is only resolved (with low residual fit) on a thin layer. This first experiment is indispensable for comforting choice of hypothesis. Upper experiments focus on SPTWS/SPTWN contributions while Lower experiments on WSPCW/PEW imply to drop a thermocline water mass.

3. Results

3.1. Entrance of the Coral Sea

3.1.1. New Caledonia-Vanuatu Channel

Because the lower thermocline in the New Caledonia-Vanuatu channel is essentially composed of WSPCW (see supporting information Figure

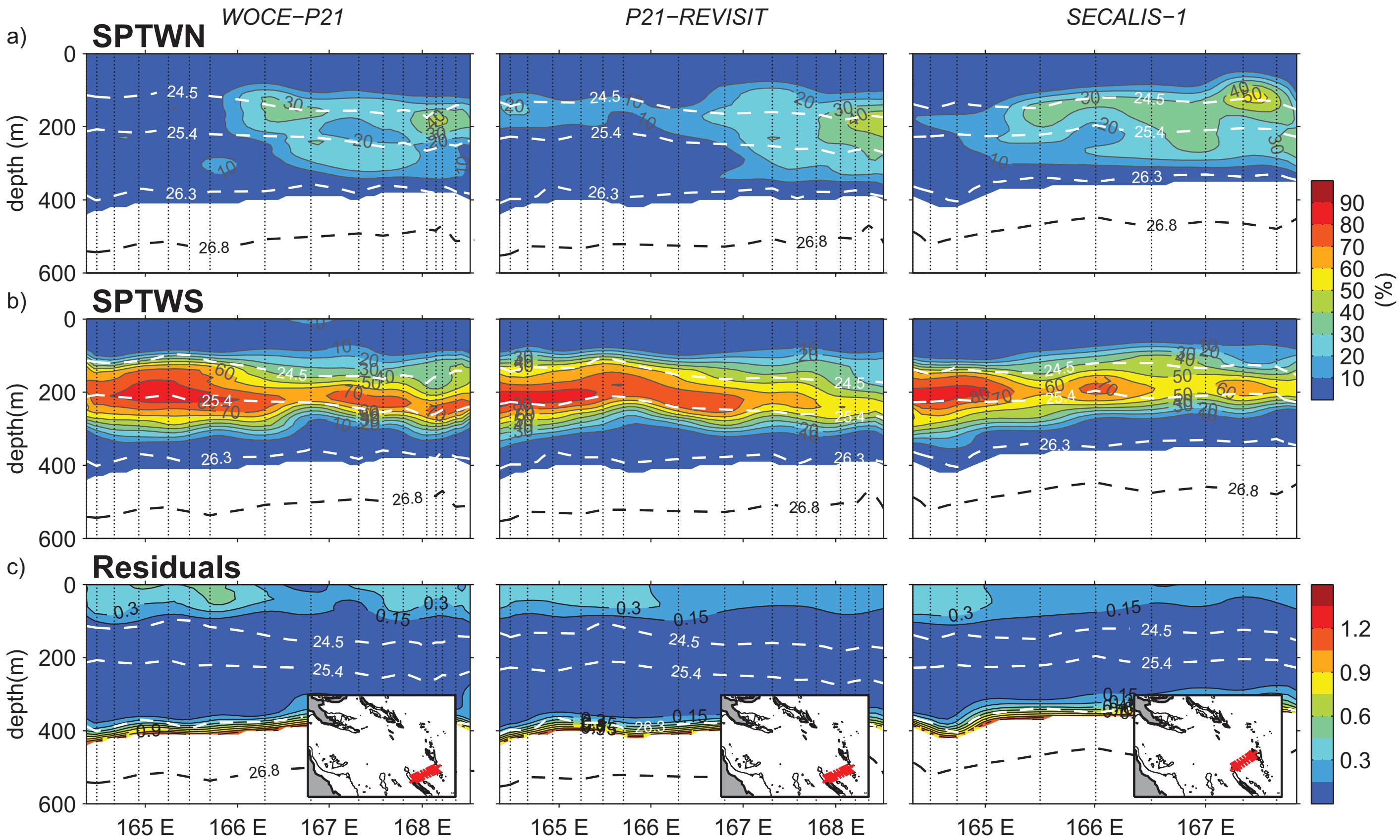

Figure 5. (a, b) Composition (in %) of the upper thermocline water masses *in the channel between New Caledonia and Vanuatu* from the WOCE-P21 (Jun 1994, inset), P21-REVISIT (Jun 2009) and SECALIS-1 (Jul 2004) cruises from the $Upper^{WSPCW}$ experiment (No PEW). TSW and AAIW are not shown because their relative contributions are low at thermocline level, and do not provide information on the water pathways. (c) Nondimensional mass residual fit. Only residual fit lower than 1.4 is shown. Key isopycnals are indicated by the dashed lines.

S8), we drop the PEW and we use the $Upper^{WSPCW}$ experiment to describe the upper thermocline composition in this area. The OMP results for sections P21 (WOCE and REVISIT) show that the SPTWS contributes more than 80% of total water column between 100 and 300 m depth (below $\sigma = 24.5$) on the three sections (Figures 5a and 5b), as suggested by the O_2 distribution (supporting information Figures S2 and S7). The SPTWS core is centered on $\sigma = 25.4$ (>80%) and located east of New Caledonia, in the East Caledonian Current (ECC) at 164–167°E [*Gasparin et al.*, 2011]. East of this, we find the SPTWN contribution (~20–30%) which is mainly supplied through the Vanuatu islands and/or by recirculation from the north [*Maes et al.*, 2007; *Ganachaud et al.*, 2008]. Slightly north of the P21 track, SECALIS-1 shows a tighter core of SPTWS near the New Caledonia coast as well as higher SPTWN contributions off the SPTWS core. This reflects the contraction of the ECC near the tip of New Caledonia at this latitude [*Gasparin et al.*, 2011]. The SPTWN contribution reflects the lower oxygen (~165 μmol kg^{-1}) and higher salinity (>35.7) observed around $\sigma = 24.5$ (supporting information Figures S2, S3, and S7). The low residuals (Figure 5c) indicate that the water content is well explained by our SWT choices between 100 m and 400 m. Above 100 m, the expected large temporal variability due to contact with the atmosphere limits the OMP diagnostics.

To distinguish WSPCW from PEW contribution in the lower thermocline, we use the $Lower^{SPTWS}$ experiment on these same sections and focus on the lower thermocline below $\sigma = 25.4$ and above $\sigma = 26.8$ (300 m to 600 m depth, Figure 6). There, WSPCW dominates, centered around $\sigma = 26.3$ with concentrations above 90% in the ECC core, near the coast of New Caledonia, where oxygen is high (supporting information Figures S2, S3, and S7) [*Gasparin et al.*, 2011]. The WSPCW horizontal extents varies: for P21-REVISIT, it occupies almost the full channel while during WOCE-P21, it is confined to the west. SECALIS-1 confirms the contraction of the ECC against the New Caledonia coast as observed in the upper thermocline. The PEW is only present at low concentration in the east of the section which suggests that the remaining contribution is a mixture of AAIW and upper thermocline water masses.

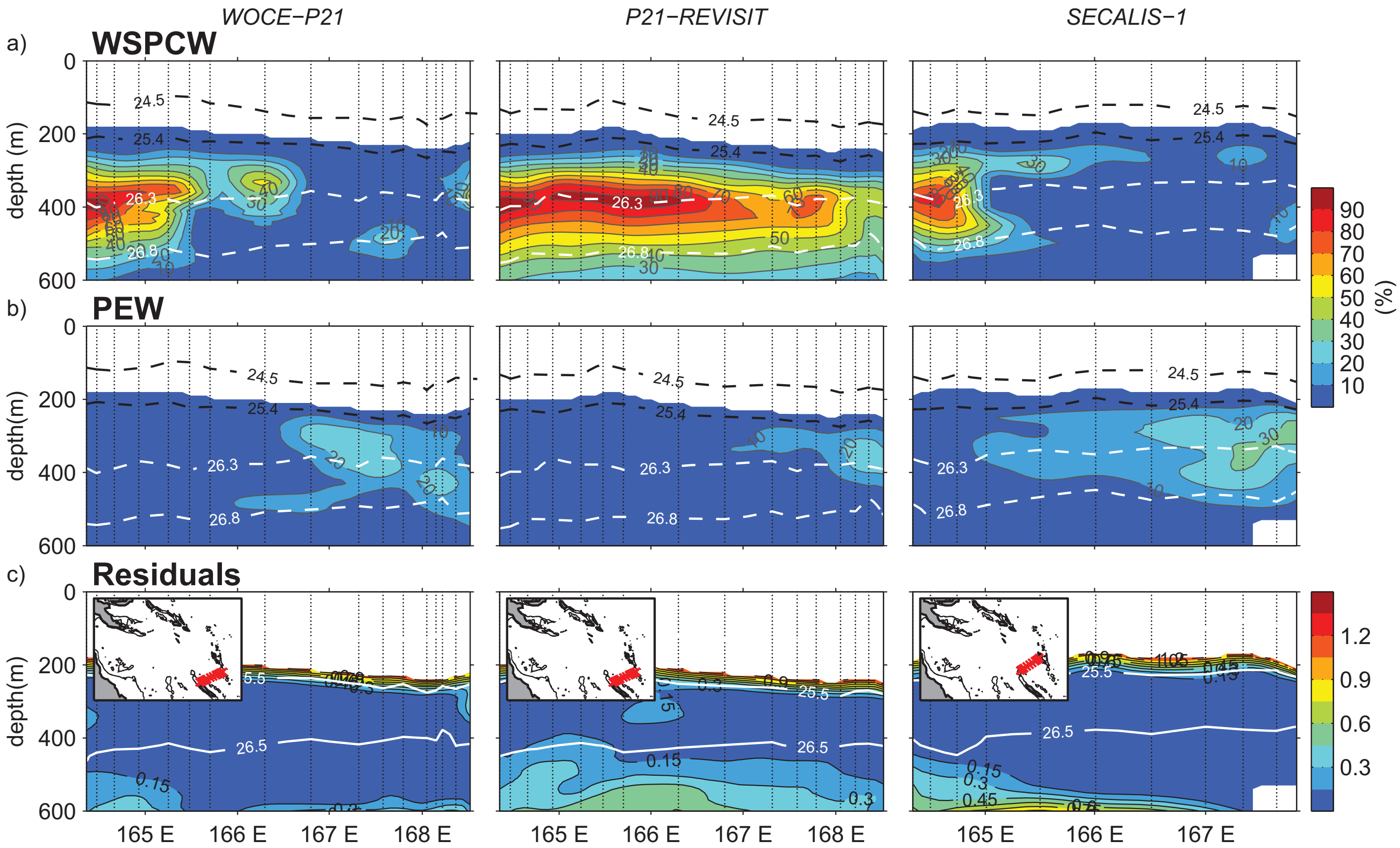

Figure 6. Same as Figure 5, but for the lower thermocline water masses from the $Lower^{SPTWS}$ experiment (No SPTWN).

This analysis in the New Caledonia-Vanuatu sections highlights that the thermocline waters are dominated by the SPTWS in the upper part and by the WSPCW in the lower part following the ECC along the coast of New Caledonia. The latter point is consistent with previous analyses reported by *Gasparin et al*. [2011]. In addition, we performed inversions along a section in the channel from the CSIRO Atlas of Regional Seas (CARS) climatology [*Ridgway and Dunn*, 2003], and confirm that SPTWS and WSPCW dominate (supporting information Figure S13). SPTWN/PEW do not appear on CARS showing that our sections show more details of the water mass distribution variability and remain consistent with CARS.

3.1.2. North of Vanuatu

North of Vanuatu, the *Mixed* experiment suggests that the WSPCW contribution is lower than the PEW contribution (and SPTWS lower than SPTWN, see supporting information Figure S9), so that we use the $Upper^{PEW}$ experiment (no WSPCW) to depict the distribution of the upper thermocline (Figure 7). The upper thermocline is mainly occupied by the SPTWN which is centered around $\sigma = 24.5$. Its highest concentrations (80%) are located north of 13°S but dominate the entire sections (>50–60%). As in the New Caledonia-Vanuatu channel (Figure 5b), the SPTWS occurs between $\sigma = 24.5$ and $\sigma = 26.3$ surfaces. Mass residuals are higher in the north, above $\sigma = 24.5$, which indicates the presence of a different, unaccounted for, SWT that probably comes from the Indispensable Strait [*Gasparin et al*., 2012].

For the lower thermocline depiction, we use the $Lower^{SPTWN}$ experiment (No SPTWS, Figure 8). Between $\sigma = 25.4$ and $\sigma = 26.8$, the WSPCW is confined south of 12°S while the PEW occupies the rest of the section. Below 500 m and north of 11°S, higher residuals indicate an equatorward change of intermediate waters properties in this area due to mixing with a deeper water mass (*Circumpolar Deep Water*), as suggested by an increasing of salinity and a decreasing of oxygen (supporting information Figures S4–S6) [*Kawabe and Fujio*, 2010].

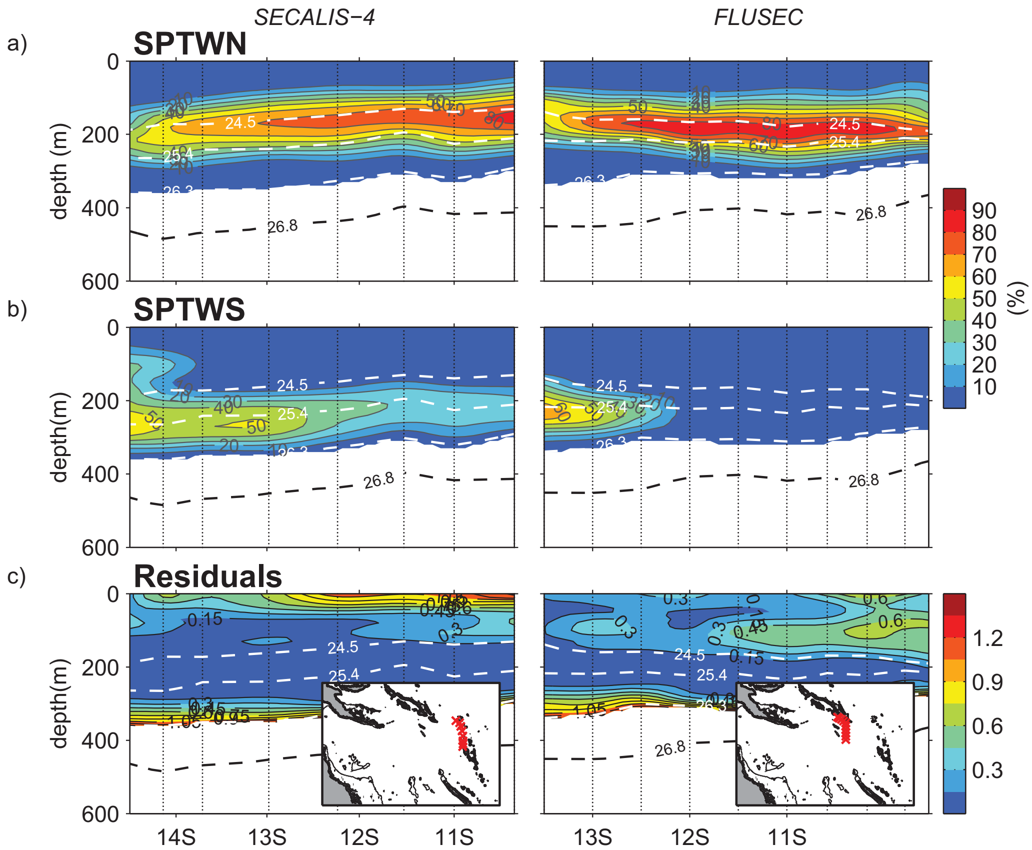

Figure 7. Same as Figure 5, but for the upper thermocline *north of Vanuatu* from SECALIS-4 (Nov 2006) and FLUSEC-1 (Aug 2007) from the *Upper*^{PEW} (No WSPCW) experiment.

Unlike in the New Caledonia-Vanuatu channel where SPTWS and WSPCW dominate thermocline waters, north of Vanuatu the thermocline is mainly constituted of SPTWN and PEW. This distribution east of the Coral Sea relates to the circulation; in the New Caledonia Vanuatu channel, the SPTWS and the WSPCW coincide with the ECC and the NCJ while north of Vanuatu the SPTWN and the PEW are located in the NVJ.

3.2. Middle of the Coral Sea

In the middle of the Coral Sea, water properties are similar to those east of the Coral Sea (supporting information Figures S4 and S5). But, because of the ubiquitous presence of two water masses at each thermocline level, we cannot ignore one to apply the *vertical stacking* strategy in this region for this section and we restrain our analysis to qualitative description. The front at around 16°S separates waters coming from the North of Vanuatu versus those from the New Caledonia channel. The SECALIS-3 section crosses the NCJ and the NVJ (Figure 1), and the *Mixed* experiment shows broad patterns in agreement with the position of the NCJ (17°S, carrying SPTWS/WSPCW) (supporting information Figure S10).

3.3. Entrance of the Solomon Sea

Around the tip of PNG, the *Mixed* inversion suggests low SPTWS contribution and high SPTWN contribution at the upper level, while around $\sigma = 26.4$, the WSPCW dominates in the NGCU with little PEW contribution. East of 155°E, SPTWN and PEW dominate (see supporting information Figure S11). To confirm this initial guess, we use the *Upper*^{WSPCW} (No PEW) and focus on NGCU waters (Figure 9). As for the *Mixed* experiment, the SPTWS contribution is low (20–30%) while SPTWN dominates (50–60%) in the upper thermocline at the tip of PNG. The residuals are higher (0.30–0.45) on the eastern end of the section, again suggesting additional, unaccounted for, contribution from Indispensable Strait.

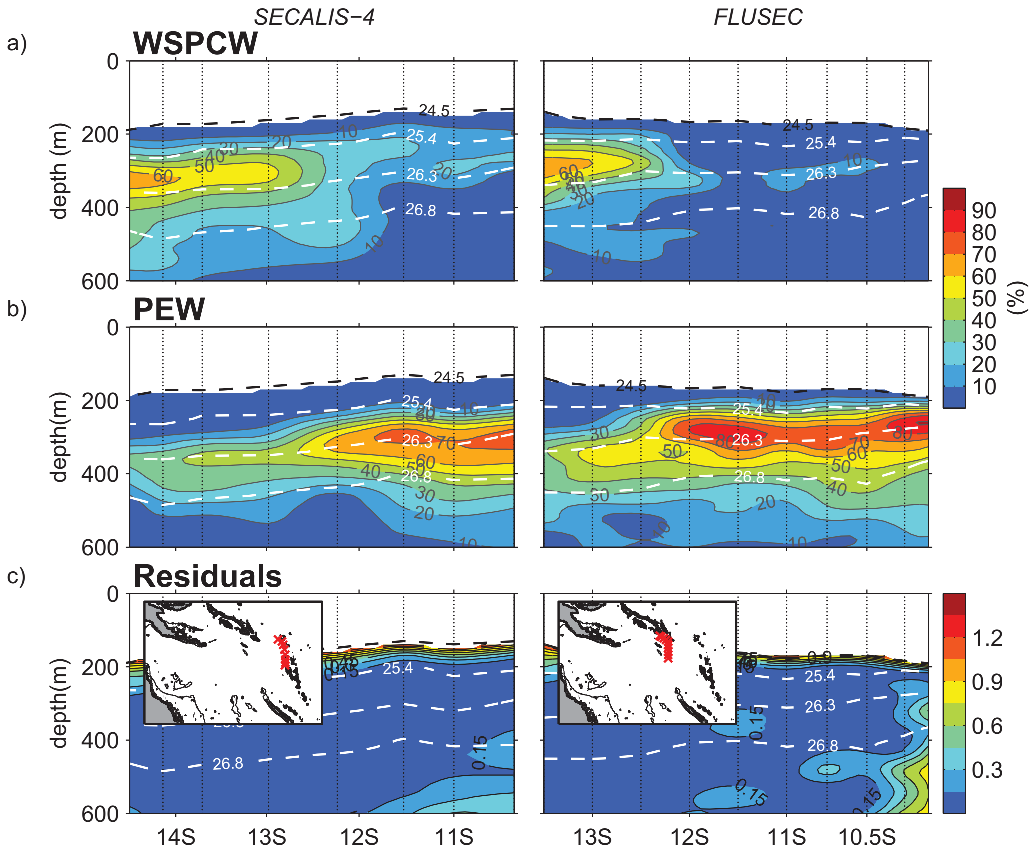

Figure 8. Same as Figure 5, but for the lower thermocline *north of Vanuatu* from the *Lower^{SPTWN}* (No SPTWS) experiment.

In the lower thermocline (*Lower^{SPTWN}*), the PEW contributions are around 20–30% while the WSPCW is higher than 50–60% around the southeast tip of PNG (Figure 10). This water mass distribution relates to the tilted bifurcation against Australian coast [*Qu and Lindstrom*, 2002; *Kessler and Cravatte*, 2013a]: in the NGCU, the upper thermocline is dominated by SPTWN coming from the NVJ, while the lower thermocline is made of WSPCW brought by the NCJ. SPTWN and PEW dominate the east part of the Solomon Sea entrance, east of 155°E in Figures 9 and 10).

On the WOCE-P11 section south of PNG, the *Mixed* experiment suggests that both SPTWS and WSPCW are located south of 16°S while a mixture of SPTWS/SPTWN is present in the upper thermocline (see supporting information Figure S12). The lower thermocline seems to be dominated by the WSPCW. The predominance of SPTWS south of 16°S is confirmed by *Upper^{WSPCW}* (Figure 11). South of PNG, SPTWS contributions are higher than during FLUSEC-1. Given the high occurrence of SPTWS in the upper thermocline, we use the *Lower^{SPTWS}* configuration (Figure 12) to diagnose the relative SWT contributions in the lower thermocline. Those are slightly different than those of the FLUSEC-1 cruise: WSPCW and PEW have similar contributions and could reflect mesoscale, interannual or decadal variability, as discussed below.

3.4. Vertical Stacking Validation and Limits

To assess the reliability of the *vertical stacking* strategy, the sum of the six water masses contributions, estimated by two different inversions depending on the section (*Upper^{WSPCW}* or *Upper^{PEW}* experiments and *Lower^{SPTWS}* or *Lower^{SPTWN}* experiments), is averaged over each section (Figure 13a). Because each inversion is independent, our description from the compilation of these experiment have residuals up to 20% of the signal at the surface and 30% between 300 and 400 m. The larger surface residual can be explained by aliasing of the atmospheric variability in the mixed layer. The 30% residual on the three sections in the NC-Vanuatu channel around 350 m is located between $\sigma = 25.4$ and $\sigma = 26.3$ at the interface between the two thermocline layers (Figure 13b, P21-REVISIT). It occurs at the water mass edges on the eastern side of the section

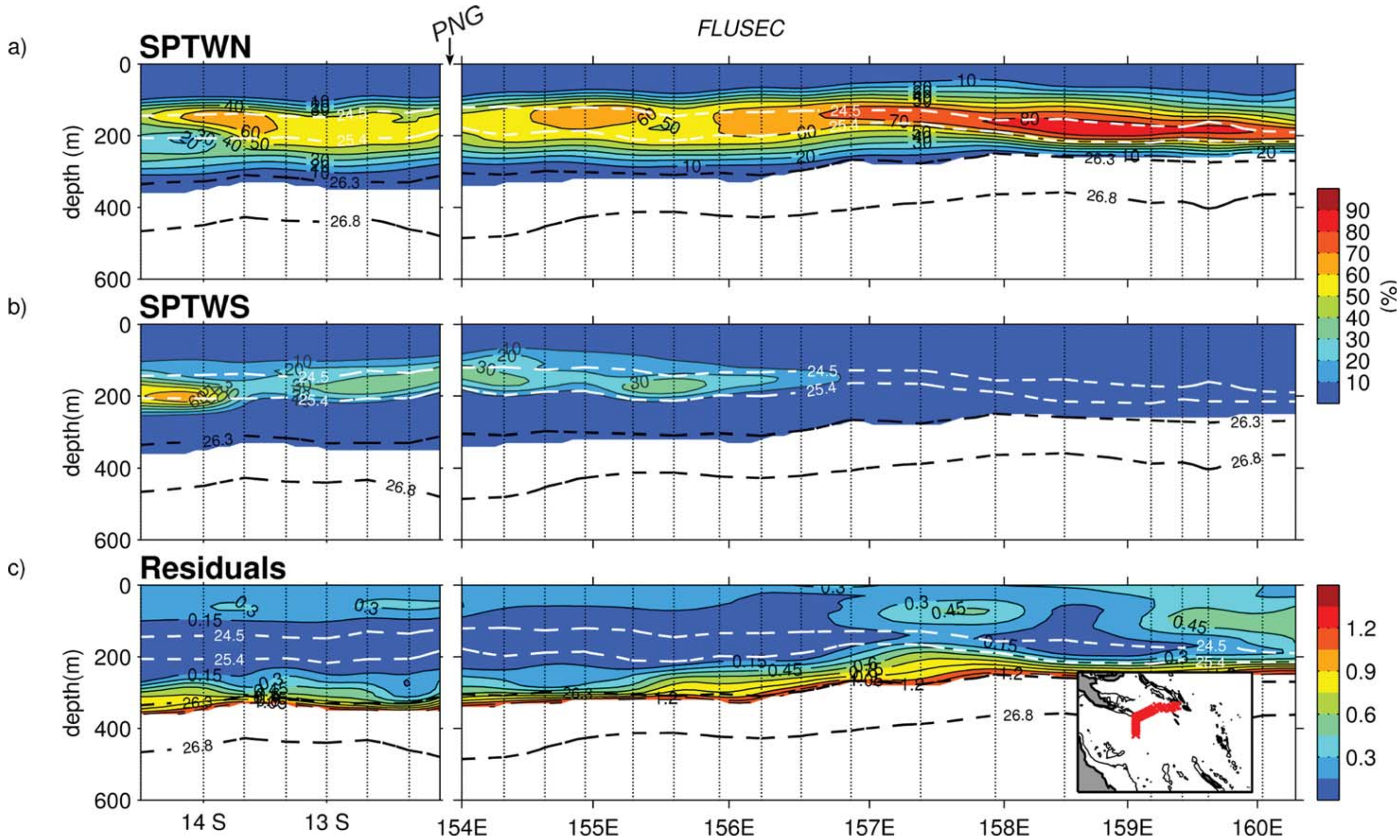

Figure 9. Same as Figure 5, but for the upper thermocline *at the entrance of the Solomon Sea* from FLUSEC-1 (Aug 2007) cruise from the *Upper*^{WSPCW} (No PEW) experiment.

due to the fact that we miss either PEW or SPTWN in *Upper*^{WSPCW} and *Lower*^{SPTWS} respectively. But, these unresolved contributions do not imply significant changes of the global scheme, and the vertical stacking has small residuals in most places over 0–600 m. Nevertheless additional parameters such as dissolved nutrients within the linear system (1) will avoid the vertical stacking hypotheses and greatly improve the resolution of the water mass distribution, in particular near the upper/lower thermocline water interface.

4. Summary and Discussion

Previous water mass descriptions in the Coral Sea were qualitatively based on Temperature-Salinity-Oxygen properties. Here an OMP analysis provides a quantitative description of the thermocline water mass distribution in relation with their pathways. Our results show distinct patterns that depend on depth/density, as summarized schematically on Figure 14. In the upper thermocline (red/green arrows), most of the SPTWN coming from the NVJ is directed equatorward, while most of the SPTWS from the NCJ is directed poleward. In the lower thermocline (blue/purple arrows), while the poleward EAC is mainly composed of WSPCW, the NGCU is composed of a mixture of the four thermocline water masses. This partition, also found in the numerical model of *Grenier et al*. [2013], reflects the tilted bifurcation of the SEC against the Australian coast [*Qu and Lindstrom*, 2002; *Kessler and Cravatte*, 2013a], with the larger influence of the lower NCJ waters and a larger influence of the upper NVJ waters.

In the eastern Coral Sea, we have shown that the SPTWS ($\sigma = 25.4$) and the WSPCW ($\sigma = 26.3$) dominate in the New Caledonia-Vanuatu channel. The corresponding cores are confined just against the east coast of New Caledonia, in the ECC (Figure 14). At the SPTWS level ($\sim\sigma = 25.3$), *Gasparin et al*. [2011] noticed that the salinity increases away from the coast of New Caledonia while oxygen concentration decreases,

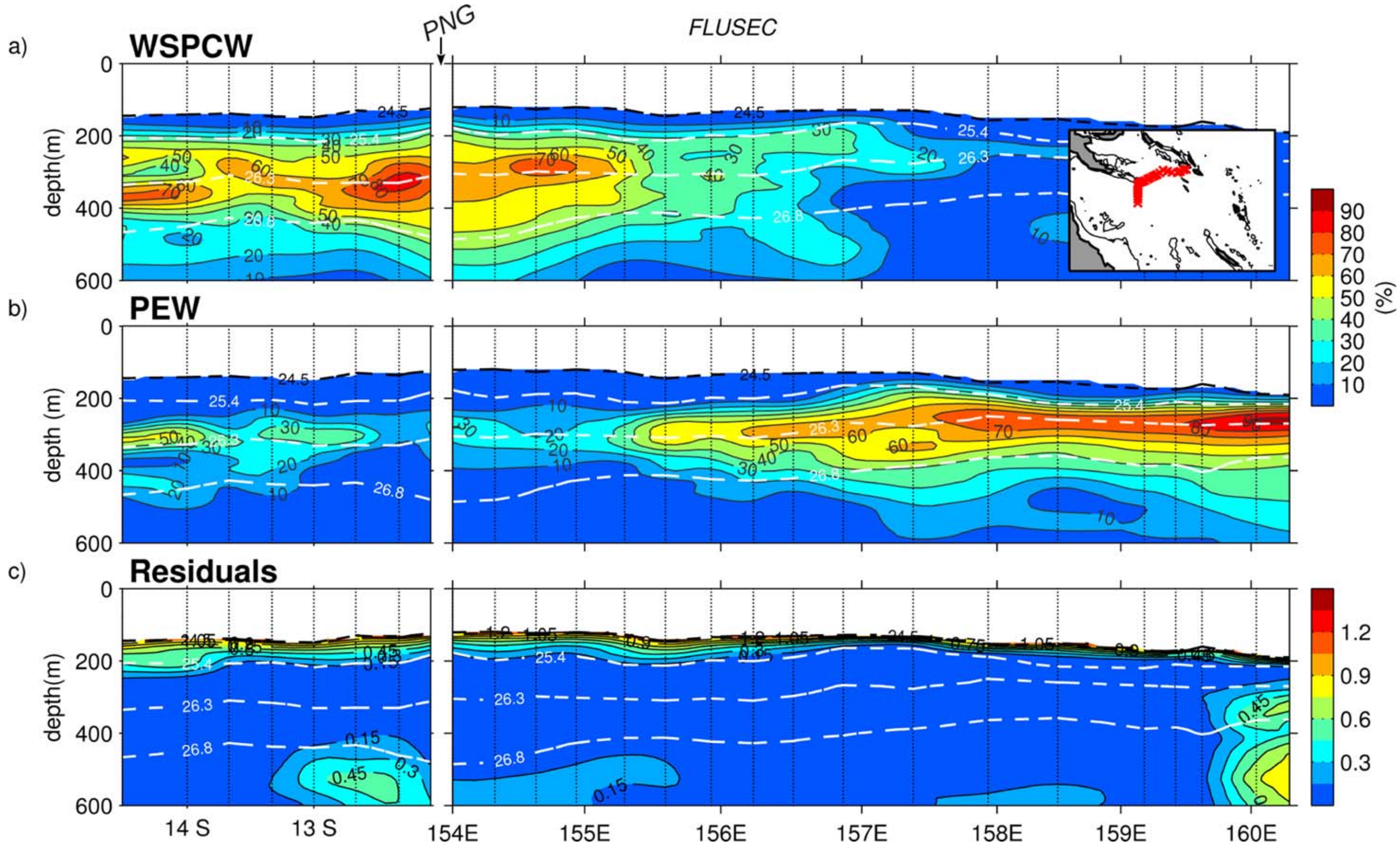

Figure 10. Same as Figure 5, but for the lower thermocline *at the entrance of the Solomon Sea* from FLUSEC-1 (Aug 2007) cruise from the *Lower*^{SPTWN} (No SPTWS) experiment.

and suspected that ECC waters are mixed with a saltier and more oxygenated water from the east. We show here that SPTWS dominates (80%) the upper thermocline in the ECC core for all sections. East of the ECC, SPTWN (20–30%) tends to erode the SPTWS core. The SPTWS horizontal extension was most significant during P21-REVISIT, consistent with a widening of the ECC at that time [*Gasparin et al*., 2011]. The *Grenier et al*. [2013] model suggested that all NCJ thermocline waters transit through the New Caledonia-Vanuatu channel, either in the ECC or through the Vanuatu islands, which is consistent with our results.

North of Vanuatu (13°S), the SPTWN ($\sigma = 24.5$) and the PEW ($\sigma = 26.3$) occupy the entire thermocline (>70%), except against the Solomon Islands where different waters could arrive through Indispensable Strait [*Gasparin et al*., 2012] (Figure 14). Between 13°S and 15°S, we find a mixture of SPTWS, SPTWN, WSCPW and PEW possibly caused by recirculations of the NCJ and NVJ [*Qiu et al*., 2009].

During FLUSEC-1, most of the upper thermocline at the entrance of the Solomon Sea in the NGCU is composed of SPTWN (more than 60% compared to 20% of SPTWS) but these contribution are reversed during WOCE-P11. This difference can be attributed to the oceanic variability, either interannual (cruises are 14 years apart) or shorter time scales as WOCE-P11 crossed a large eddy [*Kessler and Cravatte*, 2013b]. The *Grenier et al*. [2013] model analysis suggested that in the NGCU, 20% of the water came from the NCJ (~SPTWS) and 50% from the NVJ (~SPTWN), similar to our estimate during the FLUSEC-1 cruise. Such partitioning was also found using a similar OMP analysis on the CSIRO Atlas of Regional Seas (CARS) climatology [*Ridgway and Dunn*, 2003], confirming that P11 sampled an exceptional event (supporting information Figure S14).

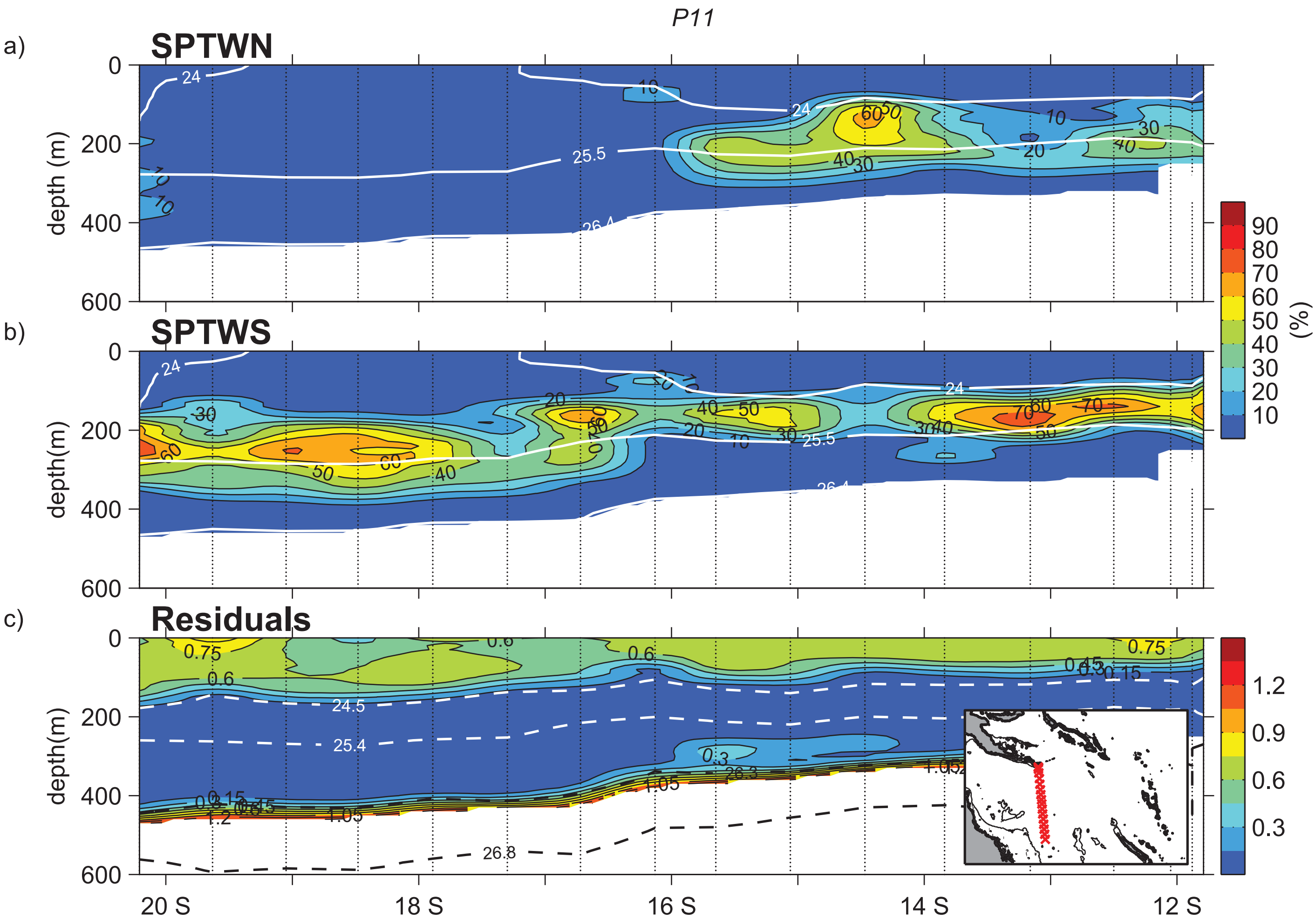

Figure 11. Same as Figure 5, but for the upper thermocline *west of the Coral Sea* from WOCE-P11 (Jun 1993) cruise from the *Upper*^{WSPCW} (No PEW) experiment.

At deeper levels, the southward shift of the NCJ bifurcation implies that a large part of WSPCW heads northward [*Qu and Lindstrom*, 2002; *Kessler and Cravatte*, 2013a] resulting in high WSPCW contributions (50–60% compared to the 20–30% of PEW) in the NGCU (Figure 14). South of 18°S, in the EAC, the WSPCW dominates with no PEW.

East of 157°E at the Solomon Sea entrance, the water mass composition is not well resolved. Southward currents have been observed in this area [*Cravatte et al*., 2011; *Davis et al*., 2012; *Gasparin et al*., 2012; *Hristova and Kessler*, 2012; *Kessler and Cravatte*, 2013a]. Besides we suspect water contributions from the Solomon Strait [*Cravatte et al*., 2011], or from the Indispensable Strait [*Gasparin et al*., 2012] which would explain the poor resolution.

In conclusion, the OMP analysis confirms the strong relationship between the water properties and jets highlighted by *Webb* [2000]. It allowed a true quantification of the respective SWT contribution, that completes the qualitative depiction solely based on water properties. Future studies should further refine this type of analysis, adding in oceanic nutrients as recently collected during SPICE, notably in the NCJ bifurcation region and inside the Solomon Sea [*Eldin et al*., 2013; Ganachaud et al., submitted manuscript, 2014]. This will enable the analysis to take into account all thermocline water masses in a single inversion instead of relying on the vertical stacking hypothesis.

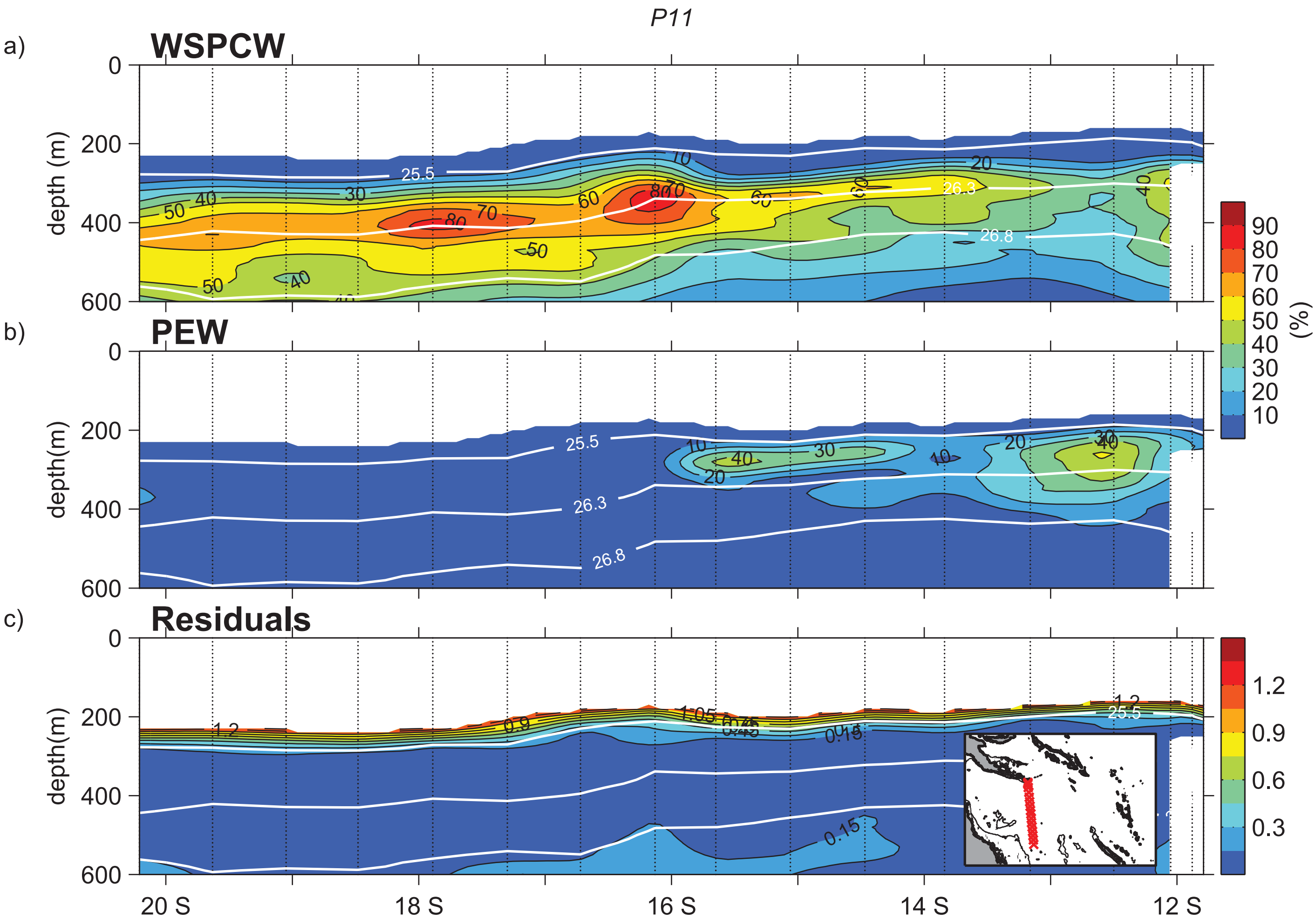

Figure 12. Same as Figure 5, but for the lower thermocline *west of the Coral Sea* from WOCE-P11 (Jun 1993) cruise from the *Lower*^{SPTWS} (No SPTWN) experiment.

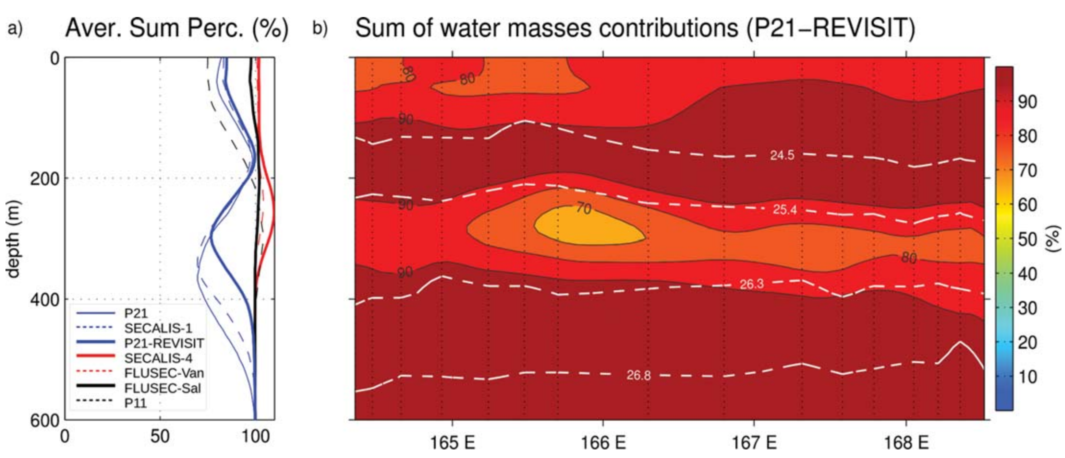

Figure 13. (a) Sum of the six water masses contribution estimated by two inversions (*vertical stacking*) depending on sections (*Upper*^{WSPCW} or *Upper*^{PEW} and *Lower*^{SPTWS} or *Lower*^{SPTWN}, see text) averaged over each section. Line colors depend on the section location: blue in the NC-Vanuatu channel, red at the north of Vanuatu and black around PNG. (b) Sum of the six water masses percentages for the P21-REVISIT section. 100% indicate that the water composition has been fully described by the SWTs from the different experiments (a unique experiment per SWT).

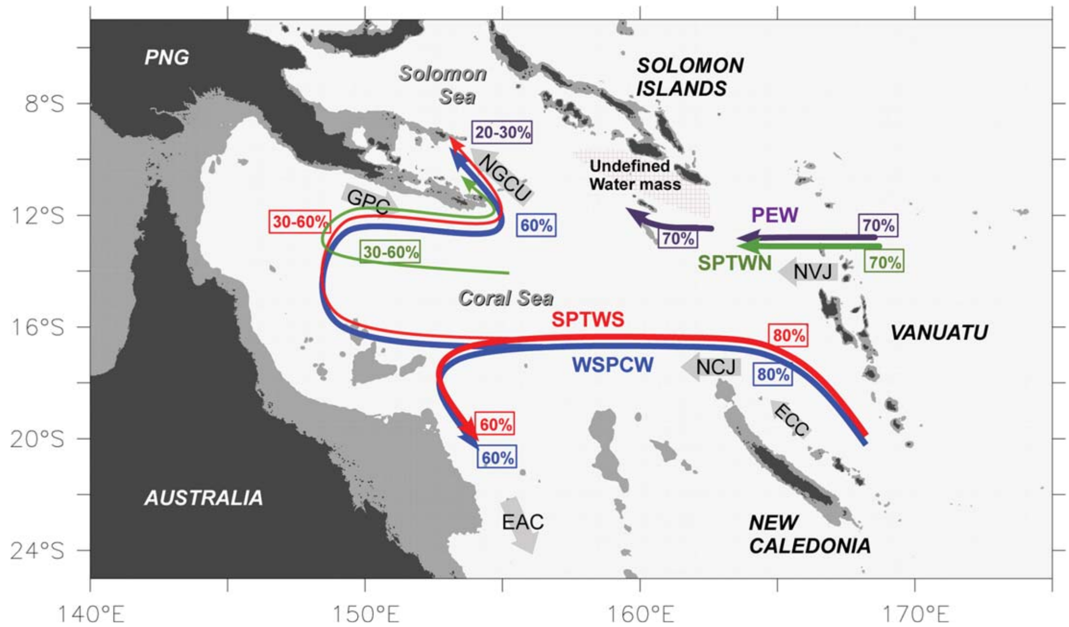

Figure 14. Upper thermocline pathways (around $\sigma = 25$, SPTWS/SPTWN, red/green arrows) and lower thermocline pathways (around $\sigma = 26.3$, WSPCW/PEW, blue/purple arrows) through the Coral Sea. Percentages indicate the mean relative contribution of each water mass at its respective thermocline level; Arrow width is proportional to these percentages. The hatched region represents an area where the thermocline composition is incomplete, and at least one more SWT would be needed. Country/Water Mass/Current names are indicated as follows: Papua New Guinea (PNG); South Pacific Tropical Water-South (SPTWS); South Pacific Tropical Water-North (SPTWN); Western South Pacific Central Water (WSPCW); Pacific Equatorial Water (PEW); East Caledonian Current (ECC); North Caledonian Jet (NCJ); North Vanuatu Jet (NVJ); Gulf of Papua Current (GPC); New Guinea Coastal Current (NGCU); East Australian Current (EAC).

Acknowledgments
The SECALIS-1, SECALIS-3, SECALIS-4, and FLUSEC-1 cruises were supported by IRD and LEGOS. The P21-REVISIT cruise was carried out by JAMSTEC. The WOCE-P11 and P21 cruises were a part of the WOCE program. We are particularly grateful to the R/V Alis crew and the IRD staff, as well as to governments of PNG, Vanuatu and the Solomon Islands. These data were collected and made freely available by the Coriolis project and programs that contribute to it (http://www.coriolis.eu.org). Melanie Grenier and Keitapu Maamaatuaiahutapu provided insightful comments. We especially thank Sophie Cravatte and Janet Sprintall for their valuable comments and suggestions. We would also like to thank two anonymous reviewers for their very thoughtful comments. This work is cofunded by ANR (ANR-09-BLAN-0233-01); INSU/LEFE/IDAO (Solwara), and the French Ministry for Education and Research (MESR); it is a contribution to the CLIVAR/SPICE International program.

References

Andrews, J. C., and S. Clegg (1989), Coral Sea circulation and transport deduced from modal information models, *Deep Sea Res., Part A*, *36*(6), 957–974.

Budillon, G., M. Pacciaroni, S. Cozzi, P. Rivaro, G. Catalano, C. Ianni, and C. Cantoni (2003), An optimum multiparameter mixing analysis of the shelf waters in the ross sea, *Antarct. Sci.*, *15*(01), 105–118.

Cravatte, S., A. Ganachaud, Q.-P. Duong, W. S. Kessler, G. Eldin, and P. Dutrieux (2011), Observed circulation in the Solomon Sea from SADCP data, *Prog. Oceanogr.*, *88*(1-4), 116–130, doi:10.1016/j.pocean.2010.12.015.

Davis, R., W. Kessler, and J. Sherman (2012), Gliders measure western boundary current transport from the south pacific to the equator, *J. Phys. Oceanogr.*, *42*, 2001–2013.

Donguy, J. R. (1994), Surface and subsurface salinity in the tropical pacific ocean: Relation with climate, *Prog. Oceanogr.*, *34*, 45–78.

Donguy, J. R., and C. Henin (1977), Origin of the surface tropical water in the Coral and Tasman seas, *Mar. Freshwater Res.*, *28*(3), 321–332.

Eldin, G., A. Ganachaud, S. Cravatte, and C. Jeandel (2013), Pandora cruise provides an unprecetented description of the Solomon Sea, *CLIVAR Exchanges*, *18*(61), 24–25.

Ganachaud, A., L. Gourdeau, and W. S. Kessler (2008), Bifurcation of the subtropical south equatorial current against New Caldeonia in December 2004 from an hydrogaphic inverse box model, *J. Phys. Oceanogr.*, *38*, 2072–2084.

Gasparin, F., A. Ganachaud, and C. Maes (2011), A western boundary current east of New Caledonia: Observed characteristics, *Deep Sea Res., Part I*, *58*(9), 956–969, doi:10.1016/j.dsr.2011.05.007.

Gasparin, F., A. Ganachaud, C. Maes, F. Marin, and G. Eldin (2012), Oceanic transports through the Solomon Sea: The bend of the New Guinea coastal undercurrent, *Geophys. Res. Lett.*, *39*, L15608, doi:10.1029/2012GL052575.

Gourdeau, L., E. Kestenare, A. Ganachaud, J.-Y. Panché, L. Jamet, A. diMatteo, J. Verron, and X. Couvelard (2007a), SECALIS-3 cruise report, 11–24 July 2005, *Rapp. de Missions, Sci. de la Mer, 21*, 80 pp.

Gourdeau, L., J. Y. Panché, D. Varillon, E. Kestenare, A. Ganachaud, J. Lefevre, P. Marchesiello, and A. Di Matteo (2007b), SECALIS-4 cruise report, 7–22 November 2006, *Rapp. de Missions, Sci. de la Mer, 23*, 80 pp.

Gourdeau, L., W. S. Kessler, R. E. Davis, J. Sherman, C. Maes, and E. Kestenare (2008), Zonal jets entering the Coral Sea, *J. Phys. Oceanogr.*, *38*(3), 715–725.

Grenier, M., C. Jeandel, F. Lacan, D. Vance, C. Venchiarutti, A. Cros, and S. Cravatte (2013), From the subtropics to the central equatorial Pacific Ocean: Neodymium isotopic composition and rare earth element concentration variations, *J. Geophys. Res. Oceans*, *118*, 592–618, doi:10.1029/2012JC008239.

Gu, D., and S. G. H. Philander (1997), Interdecadal climate fluctuations that depend on exchanges between the tropics and extratropics, *Science*, *275*(5301), 805–807.

Holbrook, N., and A. Maharaj (2008), Southwest pacific subtropical mode water: A climatology, *Prog. Oceanogr.*, *77*(4), 298–315.

Hristova, H. G., and W. S. Kessler (2012), Surface circulation in the Solomon Sea derived from Lagrangian drifter observations, *J. Phys. Oceanogr.*, *42*, 448–458, doi:10.1175/JPO-D-11-099.1.

Kawabe, M., and S. Fujio (2010), Pacific ocean circulation based on observation, *J Oceanogr*, *66*(3), 389–403, doi:10.1007/s10872-010-0034-8.

Kessler, W. S., and S. Cravatte (2013a), Mean circulation of the Coral Sea, *J. Geophys. Res. Oceans*, *118*, 6385–6410, doi:10.1002/2013JC009117.

Kessler, W. S., and S. Cravatte (2013b), ENSO and short-term variability of the south equatorial current entering the Coral Sea, *J. Phys. Oceanogr.*, *43*(5), 956–969, doi:10.1175/JPO-D-12–0113.1.

Maamaatuaiahutapu, K., V. C. Garçon, C. Provost, M. Boulahdid, and A. P. Osiroff (1992), Brazil-Malvinas confluence: Water mass composition, *J. Geophys. Res.*, *97*(C6), 9493–9505.

Mackas, D. L., K. L. Denman, and A. F. Bennett (1987), Least squares multiple tracer analysis of water mass composition, *J. Geophys. Res.*, *92*(C3), 2907–2918.

Maes, C., L. Gourdeau, X. Couvelard, and A. Ganachaud (2007), What are the origins of the Antarctic intermediate waters transported by the North Caledonian jet?, *Geophys. Res. Lett.*, *34*, L21608, doi:10.1029/2007GL031546.

Maes, C., G. Eldin, A. Melet, J. Lefevre, J. Sudre, D. Varillon, A. Ganachaud, and L. Gourdeau (2008), FLUSEC-1 cruise report, 12–30 August 2007, *Rapp. de Missions, Sci. de la Mer, 24*, 80 pp.

Melet, A., L. Gourdeau, W. S. Kessler, J. Verron, and J.-M. Molines (2010), Thermocline circulation in the Solomon Sea: A modeling study, *J. Phys. Oceanogr.*, *40*(6), 1302–1319, doi:10.1175/2009JPO4264.1.

Poole, R., and M. Tomczak (1999), Optimum multiparameter analysis of the water mass structure in the Atlantic Ocean thermocline, *Deep Sea Res., Part I*, *46*(11), 1895–1921.

Qiu, B., S. Chen, and W. S. Kessler (2009), Source of the 70-day mesoscale eddy variability in the Coral Sea and the north Fiji basin, *J. Phys. Oceanogr.*, *39*, 404–420.

Qu, T., and E. Lindstrom (2002), A climatological interpretation of the circulation in the western south pacific, *J. Phys. Oceanogr.*, *32*(9), 2492–2508.

Qu, T., and E. J. Lindstrom (2004), Northward intrusion of antarctic intermediate water in the western pacific*, *J. Phys. Oceanogr.*, *34*(9), 2104–2118, doi:10.1175/1520-0485(2004)034<2104:NIOAIW>2.0.CO;2.

Qu, T., S. Gao, I. Fukumori, R. A. Fine, and E. J. Lindstrom (2009), Origin and pathway of equatorial 13°C water in the pacific identified by a simulated passive tracer and its adjoint, *J. Phys. Oceanogr.*, *39*(8), 1836–1853.

Ridgway, K. R., and J. R. Dunn (2003), Mesoscale structure of the mean east australian current system and its relationship with topography, *Prog. Oceanogr.*, *56*(2), 189–222.

Roemmich, D., and B. Cornuelle (1992), The subtropical mode waters of the south pacific ocean, *J. Phys. Oceanogr.*, *22*(10), 1178–1187.

Sokolov, S., and S. Rintoul (2000), Circulation and water masses of the southwest pacific: WOCE section p11, Papua New Guinea to Tasmania, *J. Mar. Res.*, *58*, 223–268.

Sprintall, J., and M. Tomczak (1993), On the formation of central water and thermocline ventilation in the southern hemisphere, *Deep Sea Res., Part I*, *40*(4), 827–848.

Sudre, J., V. Garcon, C. Provost, N. Sennéchael, O. Huhn, and M. Lacombe (2011), Short-term variations of deep water masses in drake passage revealed by a multiparametric analysis of the ANT-XXIII/3 bottle data, *Deep Sea Res., Part II*, *58*(25), 2592–2612.

Sverdrup, H. U., M. W. Johnson, and R. H. Fleming (1942), *The Oceans: Their Physics, Chemistry, and General Biology*, vol. 7, Prentice Hall, N. Y.

Tomczak, M., and J. S. Godfrey (2003), *Regional Oceanography: An Introduction*, 390 pp., Daya Books, Delhi.

Tomczak, M., and D. Hao (1989), Water masses in the thermocline of the Coral Sea, *Deep Sea Res., Part A*, *36*, 10,1503–10,1514.

Tomczak, M., and D. G. B. Large (1989), Optimum multiparameter analysis of mixing in the thermocline of the eastern Indian Ocean, *J. Geophys. Res.*, *94*(C11), 16,141–16,149, doi:10.1029/JC094iC11p16141.

Tsimplis, M., S. Bacon, and H. L. Bryden (1998), The circulation of the subtropical south pacific derived from hydrographic data, *J. Geophys. Res.*, *103*(C10), 21,443–21,468.

Tsubouchi, T., T. Suga, and K. Hanawa (2007), Three types of south pacific subtropical mode waters: Their relation to the large-scale circulation of the south pacific subtropical gyre and their temporal variability, *J. Phys. Oceanogr.*, *37*(10), 2478–2490, doi:10.1175/JPO3132.1.

Tsuchiya, M., R. Lukas, R. A. Fine, E. Firing, and E. Lindstrom (1989), Source waters of the pacific equatorial undercurrent, *Prog. Oceanogr.*, *23*(2), 101–147, doi:10.1016/0079–6611(89)90012-8.

Uchida, H., A. Murata, and T. Doi (2011), *WHP p21 REVISIT Data Book*, Jpn. Agency for Mar. Earth Sci. and Technol., Yokosuka.

Webb, D. J. (2000), Evidence for shallow zonal jets in the south equatorial current region of the southwest pacific, *J. Phys. Oceanogr.*, *30*(4), 706–720.

Wyrtki, K. (1962), The subsurface water masses in the western south pacific ocean, *Mar. Freshwater Res.*, *13*(1), 18–47.